Published in final edited form as:

Biochem J. 2015 March 15; 466(3): 571–585. doi:10.1042/BJ20141042.

Degradation of gap junction connexins is regulated by the interaction with Cx43-interacting protein of 75 kDa (CIP75)

Jennifer L. Kopanic[*], **Barbara Schlingmann**[†], **Michael Koval**[†], **Alan F. Lau**[‡,§,‖], **Paul L. Sorgen**[*], and **Vivian F. Su**[‡,§,1]

[*]Department of Biochemistry and Molecular Biology, University of Nebraska Medical Center, Omaha, NE 68137, U.S.A

[†]Department of Pulmonary, Allergy, and Critical Care Medicine, Emory University School of Medicine, Atlanta, GA 30322, U.S.A

[‡]Cancer Biology Program, University of Hawai'i Cancer Center, Honolulu, HI 96813, U.S.A

[§]Pacific Biosciences Research Center, University of Hawai'i at Mānoa, Honolulu, HI 96822, U.S.A

[‖]Department of Cell and Molecular Biology, John A. Burns School of Medicine, University of Hawai'i at Mānoa, Honolulu, HI 96822, U.S.A

Abstract

Connexins are a family of transmembrane proteins that form gap junction channels. These proteins undergo both proteasomal and lysosomal degradation, mechanisms that serve to regulate connexin levels. Our previous work described CIP75 [connexin43 (Cx43)-interacting protein of 75 kDa], a protein involved in proteasomal degradation, as a novel Cx43-interacting protein. We have discovered two additional connexins, connexin40 (Cx40) and connexin45 (Cx45), that interact with CIP75. Nuclear magnetic resonance (NMR) analyses identified the direct interaction of the CIP75 UBA domain with the carboxyl-terminal (CT) domains of Cx40 and Cx45. Reduction in CIP75 by shRNA in HeLa cells expressing Cx40 or Cx45 resulted in increased levels of the connexins. Furthermore, treatment with trafficking inhibitors confirmed that both connexins undergo endoplasmic reticulum-associated degradation (ERAD), and that CIP75 preferentially interacts with the connexin proteins bound for proteasomal degradation from the ER. In addition, we have also discovered that CIP75 interacts with ER-localized Cx32 in a process that is likely mediated by Cx32 ubiquitination. Thus, we have identified novel interacting connexin proteins of CIP75, indicating a role for CIP75 in regulating the levels of connexins in general, through proteasomal degradation.

[1]To whom correspondence should be addressed (barlos@hawaii.edu).

AUTHOR CONTRIBUTION

Jennifer Kopanic designed and performed the NMR experiments, interpreted the results, and wrote the manuscript. Barbara Schlingmann and Michael Koval assisted with the Cx chimera experiments. Alan Lau and Paul Sorgen provided support throughout the study and assisted in drafting and reviewing the manuscript. Vivian Su designed and performed the cellular experiments, interpreted the results and wrote the manuscript.

Keywords

connexin; CIP75; ERAD; proteasome; protein degradation

INTRODUCTION

Gap junctions are cell-to-cell channels that allow for the direct exchange of ions and low molecular mass metabolites (<1 kDa) between adherent cells via gap junctional intercellular communication (GJIC) [1]. They provide a pathway for the propagation and/or amplification of signal transduction cascades triggered by cytokines, growth factors and other cell signalling molecules, which are critical for the development and maintenance of normal cellular functions. Connexin mutations and/or aberrant GJIC have been observed in a number of human diseases, including Charcot–Marie–Tooth disease [2], oculodentodigital dysplasia [3], Clouston syndrome or keratitis-ichthyosis-deafness syndrome [4], congenital lens cataracts [5] and cardiac arrhythmias [6]. Gap junction channels are created by the apposition of two connexons from adjacent cells, in which six connexin proteins form each connexon. There are 21 different human connexin isoforms named according to their molecular mass (e.g., 40 kDa isoform is Cx40) with differential spatial-temporal tissue expression [7]. For example, Cx40, Cx43 and Cx45 are found in distinct combinations and relative quantities in different, functionally specialized subsets of cardiomyocytes. In the diseased heart, expression levels of these cardiac connexins are altered, which can lead to abnormal impulse propagation and generation of ventricular arrhythmias, predisposing patients to heart failure [6,8].

Connexins are tetra-spanning proteins with two extracellular loops, an intracellular loop and amino- and carboxyl-termini. Even though a significant amount of sequence homology exists between connexins, the major divergence in primary structure occurs in the cytoplasmic loop and carboxyl-terminus (CT) domains, which help confer specific regulatory properties on each isoform. The CT domain plays a role in the trafficking, size, localization and turnover of gap junctions, as well as the level of intercellular coupling via numerous post-translational modifications and protein–protein interactions [9]. We have previously used NMR to assign the resonances of the soluble Cx40CT (S251-V355), Cx43CT (S255-I382) and Cx45CT (K265-I396) domains; specific sites and binding affinities of protein–protein interactions can be determined using these resonance assignments. In addition, previously published NMR studies determined that these connexins are predominantly intrinsically disordered in structure [10–14]. Intrinsically disordered proteins have many described characteristics, including protein–protein binding, flexibility and post-translational modifications [15–17]. An intrinsically disordered connexin CT domain would be ideal for cell signalling events by allowing many different binding partners with both high specificity and low affinity to rapidly switch between molecular partners, thereby activating alternative signalling pathways [15,16]. Many of the investigated connexin-interacting proteins (reviewed in [18]) bind to the disordered areas in the connexin CT domain (e.g., zonula occludins-1 [9,18]).

Despite being transmembrane proteins, connexins are highly labile with a half-life ranging from 1.5 to 5 h [19–23]. Connexins have been found to be regulated by proteasomal, lysosomal and autophagosomal degradation mechanisms (reviewed in [24,25]). We have previously reported the novel interaction between Cx43 and CIP75, a member of the ubiquitin-like (UbL)-ubiquitin-associated (UBA) domain family [26,27]. UbL-UBA proteins are involved in various processes and participate in mediating the proteasomal degradation of a number of substrates [28]. CIP75 mediates the proteasomal degradation of Cx43 via ERAD by facilitating the interaction of Cx43 with the proteasome [27,29]. Notably, this interaction does not require prior ubiquitination of Cx43 [26,30], as is typically found on proteins targeted for proteasomal degradation, such as Cx32 and Cx50 [31,32].

In the present study, we have discovered novel interactions between CIP75 and the gap junction proteins Cx40, Cx45 and Cx32. The UBA domain of CIP75 interacted directly with the CT domain of both Cx40 and Cx45. CIP75 regulates the protein levels of Cx40 and Cx45, as evidenced by increased amounts of these connexins in cells in which CIP75 levels were experimentally reduced. CIP75 exhibited an increased affinity for Cx40 and Cx45 localized in the ER and bound for proteasomal degradation, and complexes also containing proteasomal protein were detected. CIP75 also interacts with a posttranslationally modified form of Cx32 localized to the ER. Thus, CIP75 is likely a general connexin-interacting protein, regulating connexin levels by mediating proteasomal degradation.

EXPERIMENTAL PROCEDURES

Production of recombinant proteins

The UBA domain of CIP75 (M549-S596) [26], Cx32CT (C217-C283) [33], Cx37CT (C233-V333) [34], Cx40CT (S251-V355) [10], Cx43CT (S255-I382) [35], Cx45CT (K265-I396) [13] and the Cx45CT dimerization domain (A333-N361) [12] were expressed and purified as previously described. For the UBA and Cx32CT domains, site-directed mutagenesis was performed to change the linker amino acid Leu3 to Trp in order to more precisely determine the protein concentration; using circular dichroism and NMR, no change in structure was observed in either of these constructs (data not shown).

NMR analyses

^{15}N-Heteronuclear single quantum correlation (^{15}N-HSQC) NMR data were acquired using a 600-MHz Varian INOVA spectrometer outfitted with a cold probe at the University of Nebraska Medical Center's NMR Facility. NMR spectra were processed with NMRPipe and NMRDraw [36] and analysed with NMRView [37]. Gradient-enhanced ^{15}N-HSQC experiments were used to determine protein–protein interactions. For these studies, an unlabelled protein was titrated into a PBS buffer solution (pH 5.8) containing ^{15}N-labelled protein, and ^{15}N-HSQC spectra were acquired. Interactions were identified and mapped using the resonance assignments for the CIP75 UBA [26], Cx40CT [11], Cx45CT [13] and Cx43CT [35] domains. Previously collected ^{15}N-HSQC spectra of either Cx40CT, Cx45CT or Cx43CT in the presence of increased amounts of salt, BSA or calcium were used as controls to determine chemical shifts susceptible to non-specific effects [12,38]. The dissociation constants (K_d) for the Cx40CT-UBA, Cx45CT-UBA and Cx43CT-UBA

interactions were calculated by holding the concentration of the ^{15}N-labelled connexin CT domain constant (100 μM) and titrating the unlabelled CIP75 UBA domain from 0 to 1600 μM (1:0, 1:1.5, 1:3, 1:6, 1:12 and 1:16 for Cx40CT; 1:0, 1:0.25, 1:1.25, 1:2.5, 1:3.75, 1:6.25, 1:8.75, 1:12.5 and 1:16 for Cx45; 1:0, 1:1, 1:2, 1:4, 1:6, 1:8, 1:10 and 1:12 for Cx43). All titrations were used to calculate the K_d values, but not included in the figures for easier visualization of changes in the chemical shift. The decreasing signal intensity for connexin CT residues affected as a result of the increasing UBA concentrations were fit according to the nonlinear least squares method using GraphPad Prism 5.0. All values were confirmed by calculating the K_d in the same manner using ^{15}N-labelled UBA at 100 μM in the absence or presence of various concentrations of connexin CT domain. These data were calculated using at least six representative residues affected in the protein–protein interaction spectra and are reported as the mean ± S.D.

Cell culture, inhibitor treatments and shRNA knockdown of CIP75

Human cervical carcinoma (HeLa) cells (that do not express connexins), HeLa cells stably expressing chicken Cx45 (HeLa-Cx45) [39], Cx40 (HeLa-Cx40) [40] or ER-localized Cx40 (HeLa-Cx40 tagged with His-Lys-Lys-Ser-Leu, hereafter referred to as the HKKSL tag) [40] were cultured in high glucose Dulbecco's modified Eagle's medium (Gibco) supplemented with 10% fetal bovine serum, 20 mM L-glutamine, 100 U/ml of penicillin and 100 μg/ml of streptomycin at 37°C with 5% CO_2. Transient transfections were conducted using Lipofectamine 3000 (Invitrogen). Transfected cells were harvested 24–48 h after transfection.

To induce ER accumulation, protein misfolding and/or inhibit proteasomal degradation, cells were grown to confluence, treated with either 6 μg/ml of the fungal metabolite brefeldin A (BFA; Sigma) for a total of 5 h, and/or the proteasome inhibitor 0.5 μM bortezomib (LC laboratories) for a total of 3 h, and/or 1.5 μM DTT (Sigma) for a total of 2 h. In the combination treatments, cells were pretreated with BFA for 2 h, bortezomib was then added for an additional 1 h, and DTT was added for another 2 h for a total of 5 h.

CIP75 knockdown was achieved using TRC/Mission shRNA constructs (Sigma) as previously described [29]. Human CIP75 validated shRNA TRCN0000007738 (shRNA-1) and TRCN0000007741 (shRNA-2) were utilized for the knockdown, and shRNA SHC007 (luciferase shRNA control plasmid) was used as the non-targeting control.

Plasmids

pcDNA-Cx32-HKKSL [41], pcDNA-Cx32/Cx43/Cx32b-HKKSL and pcDNA-Cx32/Cx43/Cx32bR133W-HKKSL plasmids [42] were used for transient transfections.

Antibodies

CIP75 monoclonal clones A333, M398 and L64 [43], Cx45 monoclonal clone P3C9 (from Dr Paul Lampe, Fred Hutchinson Cancer Research Center, Seattle, WA), Cx45 H-85 (Santa Cruz), Cx40 (Invitrogen), Cx32 monoclonal clone 5F9A9 (Life Technologies), Cx32 (Sigma), ubiquitin clone P4D1 (Santa Cruz Biotechnology), Rpn1 (S2) (Calbiochem/Millipore), HA (Santa Cruz Biotechnology), tubulin clone DM1A (Santa Cruz

Biotechnology) primary antibodies, and IRDye 680LT/800CW anti-mouse/rabbit IgG secondary antibodies (Li-Cor) and anti-mouse/rabbit IgG secondary antibodies conjugated to Alexa 488, 594 and 647 (Life Technologies) were used.

Co-immunoprecipitation and Western blotting

Co-immunoprecipitations of proteins from various HeLa cell lines were performed as previously described [29]. Clarified supernatant proteins were immunoprecipitated with the Cx40 polyclonal antibody or the Cx45 polyclonal antibody [preabsorbed on to Protein A agarose (Pierce)] for 1–2 h at 4°C. The immune complexes were collected, washed three times with 1% Triton X-100 lysis buffer (1% Triton X-100, 400 mM NaCl, 20 mM Tris/HCl, pH 8.0, 10 μg/ml leupeptin, 10 μg/ml aprotinin, 2 mM PMSF, 1 mM benzamidine, 2 mM NEM), and the proteins released from the agarose beads by boiling for 5 min in SDS-PAGE sample buffer. The proteins were resolved by SDS-PAGE (10% polyacrylamide gel) and the proteins of interest were identified by immunoblotting. Blots were imaged with the Li-Cor Odyssey scanner using Image Studio 3.1 software (Li-Cor). All co-immunoprecipitation experiments were performed a minimum of three times and representative experiments shown.

The sequential immunoprecipitation experiments were performed as previously described with minor changes [30]. Briefly, HeLa cells were transfected with pcDNA-Cx32-HKKSL, pcDNA-Cx32/Cx43/Cx32b-HKKSL and pcDNA-Cx32/Cx43/Cx32bR133W-HKKSL and collected 48 h after transfection. Clarified supernatant proteins were immunoprecipitated with the CIP75 M398 antibody (preabsorbed on to Protein G agarose) for 1–2 h at 4°C, then incubated in RIPA buffer (150 mM NaCl, 1% sodium deoxycholate, 1% Triton X-100, 0.1% SDS, 10 mM Tris, pH 7.2, 10 μg/ml leupeptin, 10 μg/ml aprotinin, 2 mM PMSF, 1 mM benzamidine, 2 mM NEM) for 1–2 h at 4°C to disrupt protein complexes. Released proteins were then immunoprecipitated with either the Cx32 or control HA antibodies, and the immune complexes were collected with Protein G agarose for 1–2 h at 4°C. The immune complexes were washed three times with RIPA buffer, and the proteins released from the agarose by boiling for 5 min in SDS-PAGE sample buffer. The proteins were analysed by SDS-PAGE and immunoblotting for ubiquitin, Cx32 or CIP75.

Laser scanning confocal microscopy

HeLa-Cx40, HeLa-Cx40HKKSL and HeLa-Cx45 cells were transiently transfected with pcDNA-Flag-CIP75. 24–48 h after transfection, HeLa-Cx45 cells treated with BFA for 5 h, and the other transfected cells were labelled as follows. Non-connexin-expressing HeLa cells were co-transfected with pcDNA-Flag-CIP75 and either pcDNA-Cx32-HKKSL, pcDNA-Cx32/Cx43/Cx32b-HKKSL or pcDNA-Cx32/Cx43/Cx32bR133W-HKKSL. All cells were fixed in cold 80% methanol/20% acetone for 30 min at −20°C and washed thrice with 0.1% Triton X-100 in PBS (PBSTx) for 5 min each. The cells were then blocked with 5% normal goat serum and 1% BSA in PBSTx for 30 min prior to incubation with rabbit Cx40, Cx45 or Cx32 antibody, mouse IgG2a CIP75 L64 antibody and mouse IgG1 calnexin antibody in blocking solution for 1 h. After three 5 min washes with PBSTx, the cells were incubated with goat anti-rabbit Alexa 594, goat anti-mouse IgG2a Alexa 488 and goat anti-mouse IgG1 Alexa 647-conjugated secondary antibodies (Life Technologies) for 1 h, then

washed three times with PBS. The cells were mounted on slides with Airvol mounting media and the subcellular localization of Cx43, CIP75 and calnexin was visualized using the Leica 63× HCX PL Apo oil immersion objective (N.A. 1.4) on a Leica TCS SP5 AOBS confocal microscope.

Statistical analyses

Image Studio 3.1, GraphPad Prism 5.0 and SigmaPlot 9.0 were used for Western blot quantification. The statistical analysis of the CIP75, Cx40 and Cx45 levels after various pharmacological treatments or shRNA transduction relative to the tubulin loading control, and the amounts of CIP75 and Rpn1 associated with Cx40 or Cx45 relative to the amount of connexin immunoprecipitated was performed using the independent Student's *t*-test. These data were represented as the fold change of the proteins under the experimental conditions compared with control cells and expressed as the mean ± S.E.M. of three or more independent experiments.

RESULTS

We have previously demonstrated that CIP75 is required for the proteasomal degradation of Cx43; increased amounts of CIP75 resulted in more Cx43 degradation while decreased CIP75 levels conversely increased Cx43 protein levels [27]. While the interaction of CIP75 with Cx43 is not dependent on the prior ubiquitination of Cx43, CIP75 is an ubiquitin-binding protein that can interact with cellular ubiquitinated proteins [30]. These cellular proteins have yet to be identified, leading us to believe that CIP75 has additional binding partners or substrates that may also be targeted for proteasomal degradation. To begin to identify these additional substrates and further elucidate the regulation of CIP75 activity, we first sought to determine whether CIP75 could interact with additional connexin proteins. Based upon the commonality that these cardiac connexins are expressed within the same cells and associate with similar protein partners [10,12,14], we tested if the UBA domain of CIP75 could interact with either Cx40 or Cx45.

The UBA domain of CIP75 directly interacts with the carboxyl-terminus of Cx40 and Cx45

^{15}N-HSQC NMR experiments were performed by titrating unlabelled CIP75 UBA domain at various molar ratios into a 1× PBS buffer solution containing either ^{15}N-labelled Cx40CT or Cx45CT at a constant concentration (100 μM). NMR spectra of Cx40CT (Figure 1A, black) or Cx45CT (Figure 1B, black) were overlaid with spectra of the CT domains in the presence of the UBA domain (Figures 1A and 1B, red). ^{15}N-Cx43CT titrated with the unlabelled UBA domain is shown for comparison (Figure 1C) [26]. The ^{15}N-HSQC spectrum is a 2D NMR experiment in which each amino acid (except proline) gives one signal (or chemical shift) that corresponds to the N–H amide group. These chemical shifts are sensitive to the chemical environment, and small changes in structure and/or dynamics can change the chemical shift of an amino acid. The data reveal that the CIP75 UBA domain directly interacted with bacterially expressed Cx40CT and Cx45CT. The disappearance of chemical shifts in relation to the concentration of UBA protein was used to calculate the K_d for each interaction (600 ± 128 μM for the Cx40CT/UBA interaction, 286 ± 59 μM for the Cx45CT/UBA interaction, and 278 ± 26 μM for the Cx43CT/UBA interaction). The

connexin CT residues that are involved in the interaction with the UBA domain were mapped on to their respective sequence (Figures 1D–1F). Notably, in the case of all three of the connexin CT domains, the interaction with the UBA domain occurs primarily within the intrinsically disordered regions. Furthermore, the Cx45CT residues that CIP75 interacts with (Q300-L331 and H363-N379; Figures 1B and 1E) flank the Cx45 dimerization domain (A333-N361) [12,13]. To confirm that the CIP75 UBA domain does not interact with the Cx45CT dimerization domain, unlabelled Cx45CT A333-N361 polypeptide at 1500 μM was added to a solution of 1× PBS (pH 5.8) containing 15N-CIP75 UBA protein (100 μM). We discovered that none of the UBA chemical shifts were affected by the Cx45 dimerization domain peptide (Supplementary Figure S1). Due to CIP75 interaction with the regions flanking the dimerization domain, we hypothesized that CIP75 binds to monomeric Cx45. We attempted to determine whether the CIP75 UBA domain interacted with Cx45CT in the monomeric and/or dimeric conformations. Unfortunately, the CIP75 UBA peptide precipitated in the solution conditions for the Cx45CT monomer conformation; thus, titration experiments to test this hypothesis were not possible. Analysis of the connexin CT amino acid sequences did not reveal any apparent consensus sequence motifs for UBA binding. However, the affinities of the interaction with the UBA domain were similar between the Cx45 and Cx43CT domains, which were more than 2-fold stronger than that of Cx40CT.

To investigate whether the CT domains of Cx40 and Cx45 interact within the same amino acids of the UBA domain as Cx43CT, we next performed NMR experiments using ^{15}N-UBA domain and unlabelled connexin CT domains. ^{15}N-HSQC experiments were performed by titrating unlabelled Cx40CT or Cx45CT domain at various molar ratios into a 1× PBS buffer solution containing ^{15}N-UBA domain at a constant concentration (100 μM; Figure 2). The affected residues were mapped to the primary sequence of the UBA domain and correspond to residues in helix 1, loop 1 and helix 3 (epitope 1). Using the program PyMol to model the previously solved three-dimensional structure of the UBA domain (PDB code 2KNZ), we designated the residues affected by the presence of the connexin CT domains in green (Figure 3). Significantly, the UBA residues strongly affected by both Cx40CT (Figures 3A and 3D) and Cx45CT (Figures 3B and 3D) are the same residues previously described for Cx43CT (Figures 3C and 3D) [26]: L558, R569, L576, I577 and G581. With the exception of G581, these residues comprise one region on the surface of the UBA domain (Figures 3A–3C). Significantly, these same residues were not affected by ubiquitin binding (Figure 3D) [26]. Thus, these residues may represent a unique connexin-interaction domain within the CIP75 UBA domain.

CIP75 promotes the degradation of Cx40 and Cx45

To determine whether CIP75 might have a role in the proteasomal degradation of the additional connexins it interacts with or whether this activity was specific to Cx43, we tested the effects of CIP75 shRNA knockdown on the levels of Cx40 and Cx45. CIP75 shRNA was transduced into HeLa cells expressing wild-type Cx40 or Cx45 using lentivirus (Figures 4A and 4C, respectively). Two CIP75 shRNAs (shRNA-1 and shRNA-2) and one control shRNA were used. Our experiments achieved partial to significant knockdown of CIP75. In the Cx40-expressing cells, shRNA-1 partially reduced CIP75 levels to 59% (± 10%, $P <$

0.01) compared with the control shRNA cells, while shRNA-2 reduced CIP75 levels to 11% (± 1.5%, $P < 0.01$). In both cases, the reduction in CIP75 resulted in increased Cx40 protein levels, with a larger increase in the more efficient knockdown (shRNA-2). Cx40 protein levels increased 1.75-fold (± 0.34, $P = 0.07$) with shRNA-1 and 3.05-fold (±1.15, $P = 0.12$) with shRNA-2 (Figure 4B). In the Cx45-expressing cells, the shRNA-1 and shRNA-2 exhibited similar behaviour where shRNA-2 achieved a larger knockdown of CIP75 (reduced to 1.7% ± 0.7%, $P < 0.01$) compared with shRNA-1 (27.7% ± 6%, $P < 0.01$) compared with the control shRNA cells. Similar to Cx40, the knockdown of CIP75 resulted in an increase in Cx45 protein levels (1.4 ± 0.09, $P < 0.01$ for shRNA-1 and 1.64 ± 0.32, $P = 0.09$ for shRNA-2) (Figure 4D). Thus, these combined results suggested that CIP75 can affect the levels of both Cx40 and Cx45.

CIP75 interacts with misfolded ER-localized Cx40 and Cx45 bound for proteasomal degradation

Cx43 trafficking through the secretory pathway and degradation of misfolded protein via ERAD has been well documented [44]. However, the degradation of other connexin family members has not been as well studied, although there have been no reports of significant alteration of the connexin life-cycle for other connexins [9]. To study whether CIP75 has a role in the ERAD of Cx40 and Cx45, we needed to establish that these connexins are also degraded via ERAD. HeLa cells expressing wild-type Cx40 were treated with BFA for 5 h to block the transport of Cx40 from the ER to the Golgi, thus, resulting in an accumulation of Cx40 in the ER compartment [9]. BFA treatment resulted in a statistically significant 1.7-fold increase in total levels of Cx40 ($P < 0.05$; Figure 5A, lane 3, and Figure 5B). DTT treatment is known to disrupt the disulfide bonds in the Cx43 extracellular loops, resulting in increased proteasomal degradation of ER-localized Cx43 due to increased misfolding [23,45]. DTT treatment for 2 h alone decreased total Cx40 levels by 20% (Figure 5A, lane 4, and Figure 5B). However, in combination with a 3 h BFA pretreatment, DTT treatment for 2 h significantly reduced the amount of cellular Cx40 compared with the cells treated with BFA alone ($P < 0.05$; Figure 5A, lanes 3 and 5, and Figure 5B), indicating the degradation of misfolded Cx40 from the ER. To block proteasomal degradation, we treated cells with the proteasomal inhibitor bortezomib for 3 h. An increase in total levels of ubiquitinated protein was observed, consistent with the inhibition of proteasomal degradation (Figure 5A, lanes 6–9). Associated with this accumulation, a modest increase in total Cx40 was observed (Figure 5A, lane 6, and Figure 5B). A combination of BFA and bortezomib (2 h pretreatment of BFA followed by an additional 3 h with bortezomib) resulted in an accumulation of Cx40 that was similar to BFA alone (Figure 5A, lane 8, and Figure 5B). The combination treatment of BFA (2 h), bortezomib (1 h), then DTT (2 h) did result in a 1.6-fold increase in Cx40 over DTT alone. Interestingly, and unexpectedly, combination treatments of bortezomib (1 h) followed by DTT (2 h) (Figure 5A, lane 7, and Figure 5B), or BFA (2 h), bortezomib (1 h), then DTT (2 h) (Figure 5A, lane 9, and Figure 5B) did not result in an accumulation of Cx40 greater than the treatments without DTT as would be expected if DTT-induced misfolded Cx40 was only being degraded via ERAD.

For Cx45, we observed some of the same trends as Cx40 with a few notable exceptions. While individual BFA and DTT treatments increased and decreased Cx45 levels,

respectively, the combined BFA/DTT treatment resulted in a greater decrease in Cx45 levels compared with DTT alone (Figure 5C, lanes 3–5, and Figure 5D). Bortezomib treatment again increased total levels of Cx45 although when combined with BFA, it had no additional effect (Figure 5C, lanes 6 and 8, and Figure 5D). Similar to Cx40, DTT treatment combined with only bortezomib or both BFA and bortezomib also unexpectedly resulted in less total levels of Cx45 (Figure 5C, lanes 7 and 9, and Figure 5D). The combination treatments were designed to induce ER-localized connexins to undergo proteasomal degradation without actually being degraded (with proteasomal inhibition) to enhance the pool of ERAD-bound connexins; the lack of accumulation suggested a possible alternative pathway of degradation. Despite the unexpected effects in the combination treatments, each chemical produced the expected effect on total protein levels of Cx40 and Cx45.

Our discovery that CIP75 mediated the interaction between Cx43 and the proteasome, specifically the Rpn1/Rpn10 subunits of the 19S regulatory particle [29], was the first observation identifying potential machinery regulating Cx43 proteasomal degradation via ERAD. Thus, we sought to determine whether CIP75 might have a function in Cx40 and Cx45 proteasomal degradation via ERAD. To study the possibility of CIP75-mediated ERAD of Cx40, we used HeLa cells expressing wild-type Cx40 or the ER-localized Cx40HKKSL and performed the pharmacological treatments to enrich the pool of Cx40 bound for ERAD. Thus, as described earlier, wild-type Cx40 cells were treated with BFA and DTT to induce the misfolding of ER-localized Cx40, but the proteasomal degradation of these proteins was inhibited with bortezomib; the ER-localized Cx40HKKSL cells were treated with only DTT and bortezomib since Cx40HKKSL is retained in the ER [40]. Cx40 was immunoprecipitated from treated and control untreated cells. While interacting CIP75 could be found in the control cells (Figure 6A, lane 2), the interaction was significantly increased in the treated cells (Figure 6A, lane 3). We quantified the amount of CIP75 and Rpn1 detected in the immunoprecipitation and normalized the amounts to the level of Cx40 that was immunoprecipitated to account for variability in the immunoprecipitation itself. For both wild-type and ER-localized (HKKSL) Cx40, there was a 7.6-fold and 3.2-fold increase in the level of associated CIP75 in treated cells. Similarly, Rpn1 was detected with higher levels found in the treated cells (3.8-fold increase for wild-type Cx40 and 2.5-fold increase for Cx40HKKSL, Figure 6A). In addition, interaction of Cx40 with CIP75 and Rpn1 increased 8-fold in the untreated ER-localized Cx40HKKSL over wild-type Cx40 (Figure 6A, lanes 4 and 5), suggesting that CIP75 was preferentially interacting with the ER-localized Cx40 protein.

When we treated HeLa-Cx45 cells similarly and immunoprecipitated Cx45, an increased level of interaction with CIP75 (2.4-fold ± 0.4) and Rpn1 (4.2-fold ± 0.5) was also observed (Figure 6B), compared with the low level of associating protein detected in the control untreated cells following the induction of ER-stress.

To confirm the interaction of Cx40 and Cx45 with CIP75 at the ER, HeLa-Cx40, HeLa-Cx40HKKSL and HeLa-Cx45 cells were transiently transfected with Flag-CIP75 and labelled with antibodies against the appropriate connexin, CIP75 and the ER resident protein calnexin. Subcellular co-localization was examined using laser scanning confocal microscopy. Overexpressed CIP75 was found to co-localize with both Cx40 and Cx45 at or

near the ER (Figures 7A and 7C, respectively). Increasing amounts of ER-localized connexin either with the HKKSL retention signal for Cx40 (Figure 7B), or by BFA treatment for Cx45 (Figure 7D), resulted in higher levels of co-localization, supporting the interaction of CIP75 and these connexins demonstrated by the biochemical co-immunoprecipitation assays.

CIP75 does not interact with the carboxyl-terminus of Cx32 or Cx37 *in vitro* but does interact with cellular Cx32

CIP75 directly interacts with Cx40, Cx45 and Cx43 [26], which are the major cardiac connexins. To determine whether CIP75 has a general role in the proteasomal degradation of connexins, we tested if the UBA domain also interacts with either the Cx32 or Cx37 CT domains. Unlike the cardiac connexins, Cx32 and Cx37 are not expressed in cardiomyocytes [46]. ^{15}N-HSQC experiments were performed with the unlabelled UBA domain (1 mM) in a 1× PBS buffer solution containing either ^{15}N-Cx32CT or 15N-Cx37CT at 100 μM. The NMR spectra of Cx32CT (Supplementary Figure S2A, black) or Cx37CT (Supplementary Figure S2B, black) were overlaid with spectra of the CT domains with the UBA domain added in the experiment (red). Additionally, ^{15}N-HSQC experiments were performed with the unlabelled Cx32CT or Cx37CT domain (1 mM) with ^{15}N-UBA domain at 100 μM (Supplementary Figures S2C and S2D, respectively). In contrast with the results for Cx40CT, Cx45CT and Cx43CT [26], no changes in the chemical shifts were observed for any of the combinations, suggesting that the Cx32CT and Cx37CT domains are unable to interact with the UBA domain. We then performed co-immunoprecipitation experiments utilizing HeLa cells transiently expressing ER-localized Cx32HKKSL [41]. Contrary to the NMR results, we detected an interaction between CIP75 and Cx32 (Figure 8A, top panel, lane 2, arrow). While we have demonstrated herein for Cx40 and Cx45, and previously for Cx43, that ubiquitination is not a prerequisite for interaction with CIP75 [26,30], Cx32 targeted for ERAD has been previously demonstrated to be ubiquitinated [31]. Thus, the ubiquitination of Cx32 may be a necessary prerequisite of CIP75 binding. To determine whether the CIP75-interacting Cx32 protein is ubiquitinated, we performed a sequential immunoprecipitation. Upon probing the Cx32 immunoprecipitate for both Cx32 and ubiquitinated protein, we detected slower migrating bands that likely correspond to ubiquitinated Cx32 (Figure 8B, middle and right panels, lanes 7 and 13, arrowheads), suggesting that CIP75 interacts with ubiquitinated Cx32. Unlike Cx40, Cx43 and Cx45, Cx32 is known to oligomerize into connexons in the ER [47]. To determine whether the oligomerization state of Cx32 might affect its interaction with CIP75, we compared our results of CIP75 interaction with Cx32HKKSL with the Cx32/Cx43 chimera proteins previously described [42]. We transiently expressed the ER-localized Cx32/43/32bR133W-HKKSL and Cx32/43/32bHKKSL chimeras which are oligomerized or monomeric, respectively [42]. CIP75 interacted with both proteins (Figure 8A, lanes 3 and 4, arrow) and ubiquitinated chimeras could be detected in the sequential immunoprecipitations (Figure 8B, right panel, lanes 15 and 17, arrowhead), indicating that the Cx32 oligomerization state does not affect interaction with CIP75. The CIP75–Cx32 interaction was confirmed by co-localization of co-transfected Flag-CIP75 and Cx32HKKSL (or the chimeras) at the ER compartment (Figures 8C–8E). Thus, results with Cx40, Cx45 and Cx32 combined with the

previously reported results with Cx43 suggested that CIP75 may represent a common element in the mechanism involving the ERAD of the connexin family.

DISCUSSION

In the present study, we demonstrate that Cx43 is not the sole connexin that can interact with CIP75. Through NMR analyses, we found that the CIP75 UBA domain directly binds to the CT domains of Cx40 and Cx45. Significantly, CIP75 can down-regulate the levels of the interacting connexins in the cell, as the experimental reduction in CIP75 expression resulted in increased Cx40 and Cx45 levels. Interestingly, CIP75 knockdown resulted in a higher increase in Cx40 levels than Cx45. CIP75 interaction with the connexins was detected by immunofluorescence microscopy studies and biochemical interaction assays. In addition, a complex containing CIP75, Rpn1 and the connexin proteins was detected. The presence of this complex was enhanced when the amount of ER-localized connexin is increased as in the case of cells expressing the ER-retained Cx40HKKSL or when ER-stress is induced in cells using DTT treatment. These results taken together with our previously published observations for Cx43 [26,27,29] indicate a role for CIP75 in facilitating connexin proteasomal degradation via ERAD.

Our current observations suggest that CIP75 may be involved in the proteasomal degradation of the connexin family through ERAD. Other members of the UbL-UBA protein family, such as Rad23 and Dsk2, have multiple substrates; thus, it is highly probable that CIP75 also has multiple substrates. This is likely the reason why CIP75 is expressed in cells lacking connexins. Our initial hypothesis postulated that CIP75 was either a general connexin-interacting protein, or that it interacted with a specific subset of connexins that share a common feature. Significantly, we observed in the present study that CIP75 did not interact directly with Cx32CT or Cx37CT via NMR, suggesting that CIP75 is not a general connexin-interacting protein. However, these experiments did not allow us to eliminate the possibility that CIP75 interacts with a different region of Cx32 and Cx37 such as the cytoplasmic loop. In addition, because the NMR experiments utilized bacterially expressed recombinant proteins, the peptides are not ubiquitinated as bacteria do not contain the ubiquitin-conjugation machinery. Our cellular interaction experiments did not support the *in vitro* results, demonstrating that CIP75 does interact with cellular Cx32. CIP75 is unlikely to interact with the Cx32 cytoplasmic domain as co-immunoprecipitation experiments utilizing another Cx32/43/32 chimera containing the Cx43 cytoplasmic loop (Cx32/43/32a; [42]) found that CIP75 interacts with this chimera (data not shown). Thus, CIP75 most likely interacts with a modified Cx32 cytoplasmic tail domain which is probably ubiquitinated and the reason for the conflicting results. The interaction between CIP75 and Cx37 with the appropriate cellular background requires further assessment to confirm that CIP75 interacts with a subset of ubiquitinated connexins. We have not been able to successfully identify a consensus CIP75-binding sequence or motif in the interacting connexins; therefore, we believe that CIP75 binding occurs in structurally similar areas of the intrinsically disordered regions of the CT domains. Interestingly, CIP75 exhibits stronger interactions with the Cx43 and Cx45 CT domains (lower K_d values), which contain more α-helical content than Cx40CT (and Cx32CT and Cx37CT, which contain less α-helical content than Cx40CT), suggesting that the secondary structure of the proteins may influence their ability to bind to

the UBA domain. An ubiquitin modification could provide a mechanism for the connexins whose secondary structure does not allow for an ubiquitin-independent interaction with CIP75 that we have observed for Cx43, Cx40 and Cx45.

It is worthwhile to note that the three connexins that do interact with CIP75 may have similar maturation and oligomerization processes. Differences between various connexins have been found in the cellular localization of oligomerization into connexons. For example, Cx43 oligomerizes in the trans-Golgi apparatus [47,48], whereas Cx32 oligomerizes in the ER [47]. A recent study proposed that certain motifs flanking the third transmembrane domain may determine where a connexin will oligomerize [40]. The R- and W-type motifs were identified and correspond to connexon oligomerization in the Golgi apparatus and ER, respectively. To complicate the picture, a number of connexins, including Cx40, lack both motifs. Interestingly, Cx43, which contains the R-motif, and Cx40 both oligomerized in the trans-Golgi apparatus. Cx45 also contains the R-motif, but its oligomerization site has not been reported. However, because CIP75 binds to residues flanking the Cx45 dimerization domain, there may be a preference for CIP75 binding to a specific form (monomer compared with dimer) of Cx45. For the connexins that are unable to interact with the CIP75 UBA domain *in vitro*, Cx32 contains the W-motif and Cx37 does not contain either motif. However, Cx37 partially oligomerizes in the ER [40], similar to Cx32 [47]. Based upon these observations, we speculate that CIP75 may specifically interact with connexins in their monomeric conformations in the ER membrane, and that the ubiquitination of connexins that normally oligomerize at the ER facilitates interaction of these larger complexes with CIP75.

From our recent observations, we would like to propose a model for CIP75 function in proteasomal degradation (Figure 9). CIP75, through the same region in the UBA domain (epitope 1), first binds to non-ubiquitinated monomeric connexins that are localized in the ER membrane, which actively facilitates the dislocation of these connexins out of the ER membrane into the cytosol. Once in the cytosol, CIP75 mediates the association with Rpn1 and Rpn10 in the 19S proteasome subunit to promote the proteasomal degradation of these connexins. Additionally, CIP75 is an ubiquitin-binding protein and can interact with cellular ubiquitinated proteins through a different region in the UBA domain [26,30]. In our model, we propose that through a different region of the UBA domain, CIP75 also binds to ubiquitinated proteins (connexins and perhaps unrelated proteins) to also mediate their proteasomal degradation. The binding affinity of CIP75 for these different substrates may mediate the activity of CIP75. Alternatively, the levels of the substrates in the ER might determine which protein CIP75 interacts with (e.g., increased levels of Cx43 in the ER due to cellular stress might increase the interaction with CIP75 to facilitate Cx43 proteasomal degradation). Based on our previous studies of misfolded Cx43 [49], the connexin protein that escapes CIP75 regulation is functional and can participate in GJIC, and can be completely folded properly or, perhaps under conditions of stress, have some degree of misfolding. We have observed that connexin protein that contains some misfolding is also able to function in GJIC, although with reduced function [49]. Notably, our results on the effect of inducing protein misfolding with DTT while blocking degradation with the proteasomal inhibitor bortezomib revealed that the proteasome may not be the only

destination for degradation of misfolded connexins. Alternative degradation of connexins that have accumulated in the ER due to BFA treatment has previously been reported where BFA treatment of breast cancer cells did not reduce the localization of Cx43 to the lysosome [50]. Thus, the degradation observed in cells treated with DTT and bortezomib could suggest the lysosomal degradation of misfolded protein. Furthermore, autophagic degradation has been reported for a number of connexins [24] and this pathway also utilizes the lysosome for protein degradation.

The interaction of Cx40, Cx43 and Cx45 with CIP75 may have implications in heart disease, as these major cardiac connexins directly interact with CIP75. In heart disease, aberrant GJIC and connexin levels or localization has been observed [6]. For example, decreased Cx43 levels have been observed after myocardial infarction, while a lateralization of Cx43 gap junctions away from intercalated disk regions occurs in arrhythmias. In addition, patients with atrial fibrillation have been found with Cx40 mutations that cause increased Cx40 proteasomal degradation [51]. Experimental therapies designed to enhance GJIC may prove to be effective treatment for heart trauma. Rotigaptide enhances GJIC and the Cx43 structural mimetic (to the first extracellular loop), gap26, protects against ischemic injury [52,53]. The ability of CIP75 to interact with the major cardiac connexins suggests that it may function as a cardiac connexin modulator. A protein such as CIP75 that is able to modulate connexin levels might thus be an alternative target for therapy. Future cellular studies of the interaction of CIP75 with connexins as well as non-connexin ubiquitinated proteins will help shape our understanding of the roles CIP75 has in the cell, and potentially, in disease.

Supplementary Material

Refer to Web version on PubMed Central for supplementary material.

Acknowledgments

We thank Dr Paul Lampe for providing the Cx45 monoclonal antibody and Drs Eric Beyer and Joanna Gemel for sharing the HeLa-Cx40 and HeLa-Cx45 cell lines. We also thank Drs Asia Gaweka and Steve Ward for technical assistance, and Ed Ezell (University of Nebraska Medical Center NMR Facility) and Sydney Zach for their discussions and technical assistance.

FUNDING

This work was supported in part by Graduate Assistance in Areas of National Need Fellowships from the U.S. Department of Education [grant number P200A070554 (to J.L.K.)], the United States Public Health Service Grant [grant number GM072631 (to P.L.S.)], the National Heart, Lung, and Blood Institute, National Institutes of Health [grant number HL116958 (to M.K.)], the American Heart Association [grant number 11POST5460028 (to V.S.)], the Hawaii Community Foundation [grant number 11ADVC-49235 (to V.S. and A.F.L.)], the National Cancer Institute, National Institutes of Health [grant number CA052098 (to A.F.L.)], the National Center for Research Resources [grant number 2G12RR003061-26 (to A.F.L.)], the National Institute on Minority Health and Health Disparities [grant number 8G12MD7601-27 (to A.F.L.)], and support from the Pacific Biosciences Research Center (to V.S. and A.F.L.).

Abbreviations

BFA	brefeldin A

CIP75	connexin43-interacting protein of 75 kDa
CT	carboxyl-terminus
Cx43	connexin43
ER	endoplasmic reticulum
ERAD	ER-associated degradation
GJIC	gap junctional intercellular communication
^{15}N-HSQC	^{15}N-heteronuclear single quantum correlation
NMR	nuclear magnetic resonance
UbL	ubiquitin-like
UBA	ubiquitin-associated

References

1. Goodenough DA, Goliger JA, Paul DL. Connexins, connexons, and intercellular communication. Annu Rev Biochem. 1996; 65:475–502. [PubMed: 8811187]
2. Nelis E, Haites N, Van Broeckhoven C. Mutations in the peripheral myelin genes and associated genes in inherited peripheral neuropathies. Hum Mutat. 1999; 13:11–28. [PubMed: 9888385]
3. Laird DW. Syndromic and non-syndromic disease-linked Cx43 mutations. FEBS Lett. 2014; 588:1339–1348. [PubMed: 24434540]
4. Berger AC, Kelly JJ, Lajoie P, Shao Q, Laird DW. Mutations in Cx30 that are linked to skin disease and non-syndromic hearing loss exhibit several distinct cellular pathologies. J Cell Sci. 2014; 127:1751–1764. [PubMed: 24522190]
5. Gerido DA, White TW. Connexin disorders of the ear, skin, and lens. Biochim Biophys Acta. 2004; 1662:159–170. [PubMed: 15033586]
6. Severs NJ, Bruce AF, Dupont E, Rothery S. Remodelling of gap junctions and connexin expression in diseased myocardium. Cardiovasc Res. 2008; 80:9–19. [PubMed: 18519446]
7. Nielsen MS, Nygaard Axelsen L, Sorgen PL, Verma V, Delmar M, Holstein-Rathlou NH. Gap junctions. Compr Physiol. 2012; 2:1981–2035. [PubMed: 23723031]
8. van Veen AA, van Rijen HV, Opthof T. Cardiac gap junction channels: modulation of expression and channel properties. Cardiovasc Res. 2001; 51:217–229. [PubMed: 11470461]
9. Laird DW. Life cycle of connexins in health and disease. Biochem J. 2006; 394:527–543. [PubMed: 16492141]
10. Bouvier D, Kieken F, Kellezi A, Sorgen PL. Structural changes in the carboxyl terminus of the gap junction protein connexin 40 caused by the interaction with c-Src and zonula occludens-1. Cell Commun Adhes. 2008; 15:107–118. [PubMed: 18649183]
11. Bouvier D, Kieken F, Sorgen PL. (1)H, (13)C, and (15)N backbone resonance assignments of the carboxyl terminal domain of Connexin40. Biomol NMR Assign. 2007; 1:155–157. [PubMed: 19636853]
12. Kopanic JL, Al-Mugotir MH, Kieken F, Zach S, Trease AJ, Sorgen PL. Characterization of the connexin45 carboxyl-terminal domain structure and interactions with molecular partners. Biophys J. 2014; 106:2184–2195. [PubMed: 24853747]
13. Kopanic JL, Sorgen PL. Chemical shift assignments of the connexin45 carboxyl terminal domain: monomer and dimer conformations. Biomol NMR Assign. 2013; 7:293–297. [PubMed: 23070843]
14. Sorgen PL, Duffy HS, Sahoo P, Coombs W, Delmar M, Spray DC. Structural changes in the carboxyl terminus of the gap junction protein connexin43 indicates signaling between binding

domains for c-Src and zonula occludens-1. J Biol Chem. 2004; 279:54695–54701. [PubMed: 15492000]

15. Cumberworth A, Lamour G, Babu MM, Gsponer J. Promiscuity as a functional trait: intrinsically disordered regions as central players of interactomes. Biochem J. 2013; 454:361–369. [PubMed: 23988124]
16. Dunker AK, Brown CJ, Lawson JD, Iakoucheva LM, Obradovic Z. Intrinsic disorder and protein function. Biochemistry. 2002; 41:6573–6582. [PubMed: 12022860]
17. Gao J, Xu D. Correlation between posttranslational modification and intrinsic disorder in protein. Pac Symp Biocomput. 2012:94–103. [PubMed: 22174266]
18. Herve JC, Bourmeyster N, Sarrouilhe D, Duffy HS. Gap junctional complexes: from partners to functions. Prog Biophys Mol Biol. 2007; 94:29–65. [PubMed: 17507078]
19. Beardslee MA, Laing JG, Beyer EC, Saffitz JE. Rapid turnover of connexin43 in the adult rat heart. Circ Res. 1998; 83:629–635. [PubMed: 9742058]
20. Darrow BJ, Laing JG, Lampe PD, Saffitz JE, Beyer EC. Expression of multiple connexins in cultured neonatal rat ventricular myocytes. Circ Res. 1995; 76:381–387. [PubMed: 7859384]
21. Fallon RF, Goodenough DA. Five-hour half-life of mouse liver gap-junction protein. J Cell Biol. 1981; 90:521–526. [PubMed: 7287816]
22. Laird DW, Puranam KL, Revel JP. Turnover and phosphorylation dynamics of connexin43 gap junction protein in cultured cardiac myocytes. Biochem J. 1991; 273:67–72. [PubMed: 1846532]
23. Musil LS, Le AC, VanSlyke JK, Roberts LM. Regulation of connexin degradation as a mechanism to increase gap junction assembly and function. J Biol Chem. 2000; 275:25207–25215. [PubMed: 10940315]
24. Su V, Lau AF. Connexins: mechanisms regulating protein levels and intercellular communication. FEBS Lett. 2014; 588:1212–1220. [PubMed: 24457202]
25. Thevenin AF, Kowal TJ, Fong JT, Kells RM, Fisher CG, Falk MM. Proteins and mechanisms regulating gap-junction assembly, internalization, and degradation. Physiology. 2013; 28:93–116. [PubMed: 23455769]
26. Kieken F, Spagnol G, Su V, Lau AF, Sorgen PL. NMR structure note: UBA domain of CIP75. J Biomol NMR. 2010; 46:245–250. [PubMed: 20127391]
27. Li X, Su V, Kurata WE, Jin C, Lau AF. A novel connexin43-interacting protein, CIP75, which belongs to the UbL-UBA protein family, regulates the turnover of connexin43. J Biol Chem. 2008; 283:5748–5759. [PubMed: 18079109]
28. Su V, Lau AF. Ubiquitin-like and ubiquitin-associated domain proteins: significance in proteasomal degradation. Cell Mol Life Sci. 2009; 66:2819–2833. [PubMed: 19468686]
29. Su V, Hoang C, Geerts D, Lau AF. CIP75 (connexin43-interacting protein of 75 kDa) mediates the endoplasmic reticulum dislocation of connexin43. Biochem J. 2014; 458:57–67. [PubMed: 24256120]
30. Su V, Nakagawa R, Koval M, Lau AF. Ubiquitin-independent proteasomal degradation of endoplasmic reticulum-localized connexin43 mediated by CIP75. J Biol Chem. 2010; 285:40979–40990. [PubMed: 20940304]
31. Kelly SM, VanSlyke JK, Musil LS. Regulation of ubiquitin-proteasome system mediated degradation by cytosolic stress. Mol Biol Cell. 2007; 18:4279–4291. [PubMed: 17699585]
32. Minogue PJ, Beyer EC, Berthoud VM. A connexin50 mutant, CX50fs, that causes cataracts is unstable, but is rescued by a proteasomal inhibitor. J Biol Chem. 2013; 288:20427–20434. [PubMed: 23720739]
33. Stauch K, Kieken F, Sorgen P. Characterization of the structure and intermolecular interactions between the connexin 32 carboxyl-terminal domain and the protein partners synapse-associated protein 97 and calmodulin. J Biol Chem. 2012; 287:27771–27788. [PubMed: 22718765]
34. Nelson TK, Sorgen PL, Burt JM. Carboxy terminus and pore-forming domain properties specific to Cx37 are necessary for Cx37-mediated suppression of insulinoma cell proliferation. Am J Physiol Cell Physiol. 2013; 305:C1246–1256. [PubMed: 24133065]
35. Sorgen PL, Duffy HS, Cahill SM, Coombs W, Spray DC, Delmar M, Girvin ME. Sequence-specific resonance assignment of the carboxyl terminal domain of Connexin43. J Biomol NMR. 2002; 23:245–246. [PubMed: 12238598]

36. Delaglio F, Grzesiek S, Vuister GW, Zhu G, Pfeifer J, Bax A. NMRPipe: a multidimensional spectral processing system based on UNIX pipes. J Biomol NMR. 1995; 6:277–293. [PubMed: 8520220]
37. Johnson BA, Blevins RA. NMR view: a computer program for the visualization and analysis of NMR data. J Biomol NMR. 1994; 4:603–614. [PubMed: 22911360]
38. Bouvier D, Spagnol G, Chenavas S, Kieken F, Vitrac H, Brownell S, Kellezi A, Forge V, Sorgen PL. Characterization of the structure and intermolecular interactions between the connexin40 and connexin43 carboxyl-terminal and cytoplasmic loop domains. J Biol Chem. 2009; 284:34257–34271. [PubMed: 19808665]
39. Elenes S, Martinez AD, Delmar M, Beyer EC, Moreno AP. Heterotypic docking of Cx43 and Cx45 connexons blocks fast voltage gating of Cx43. Biophys J. 2001; 81:1406–1418. [PubMed: 11509355]
40. Smith TD, Mohankumar A, Minogue PJ, Beyer EC, Berthoud VM, Koval M. Cytoplasmic amino acids within the membrane interface region influence connexin oligomerization. J Membr Biol. 2012; 245:221–230. [PubMed: 22722762]
41. Das Sarma J, Wang F, Koval M. Targeted gap junction protein constructs reveal connexin-specific differences in oligomerization. J Biol Chem. 2002; 277:20911–20918. [PubMed: 11929864]
42. Maza J, Das Sarma J, Koval M. Defining a minimal motif required to prevent connexin oligomerization in the endoplasmic reticulum. J Biol Chem. 2005; 280:21115–21121. [PubMed: 15817491]
43. Su V, Knutson A, Lau K, Kurata W, Berestecky J, Lau AF. Generation and characterization of mouse monoclonal antibodies against CIP75, an UbL-UBA domain-containing protein. Hybridoma (Larchmt). 2009; 28:79–84. [PubMed: 19249996]
44. Su V, Lau AF. Ubiquitination, intracellular trafficking, and degradation of connexins. Arch Biochem Biophys. 2012; 524:16–22. [PubMed: 22239989]
45. VanSlyke JK, Musil LS. Dislocation and degradation from the ER are regulated by cytosolic stress. J Cell Biol. 2002; 157:381–394. [PubMed: 11980915]
46. Kato T, Iwasaki YK, Nattel S. Connexins and atrial fibrillation: filling in the gaps. Circulation. 2012; 125:203–206. [PubMed: 22158757]
47. Das S, Smith TD, Sarma JD, Ritzenthaler JD, Maza J, Kaplan BE, Cunningham LA, Suaud L, Hubbard MJ, Rubenstein RC, Koval M. ERp29 restricts Connexin43 oligomerization in the endoplasmic reticulum. Mol Biol Cell. 2009; 20:2593–2604. [PubMed: 19321666]
48. Musil LS, Goodenough DA. Multisubunit assembly of an integral plasma membrane channel protein, gap junction connexin43, occurs after exit from the ER. Cell. 1993; 74:1065–1077. [PubMed: 7691412]
49. Dunn CA, Su V, Lau AF, Lampe PD. Activation of Akt, not connexin 43 protein ubiquitination, regulates gap junction stability. J Biol Chem. 2012; 287:2600–2607. [PubMed: 22139843]
50. Qin H, Shao Q, Igdoura SA, Alaoui-Jamali MA, Laird DW. Lysosomal and proteasomal degradation play distinct roles in the life cycle of Cx43 in gap junctional intercellular communication-deficient and -competent breast tumor cells. J Biol Chem. 2003; 278:30005–30014. [PubMed: 12767974]
51. Gemel J, Simon AR, Patel D, Xu Q, Matiukas A, Veenstra RD, Beyer EC. Degradation of a connexin40 mutant linked to atrial fibrillation is accelerated. J Mol Cell Cardiol. 2014; 74:330–339. [PubMed: 24973497]
52. Herve JC, Dhein S. Peptides targeting gap junctional structures. Curr Pharm Des. 2010; 16:3056–3070. [PubMed: 20687876]
53. Herve JC, Dhein S. Pharmacology of cardiovascular gap junctions. Adv Cardiol. 2006; 42:107–131. [PubMed: 16646587]

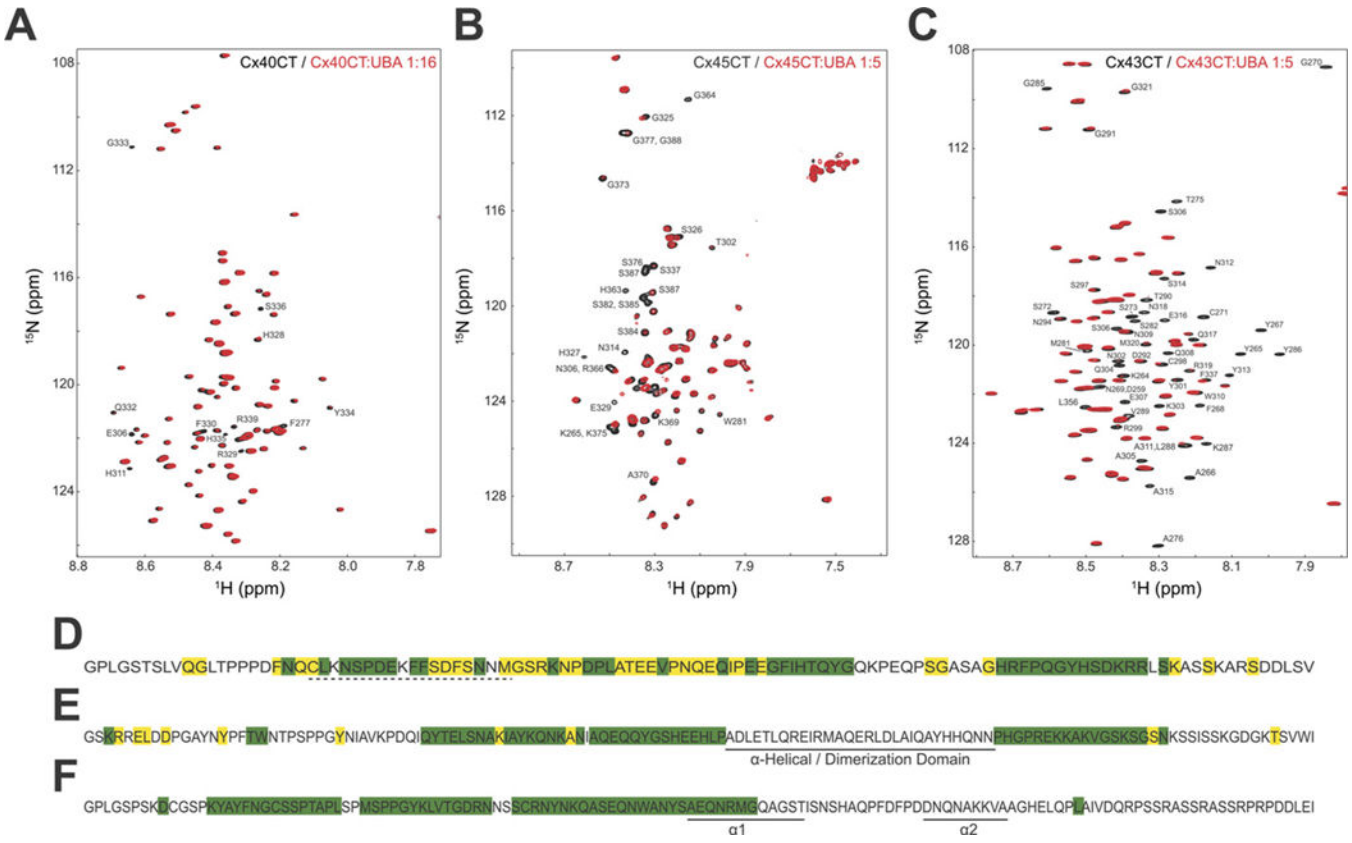

Figure 1. Cx40CT, Cx45CT and Cx43CT directly interact with the CIP75 UBA domain

(**A**) ^{15}N-HSQC titration of ^{15}N-Cx40CT with the unlabelled CIP75 UBA domain, where the Cx40CT:UBA domain concentration ratios ranged from 1:0 to 1:16 and concentration of ^{15}N-Cx40CT remained constant (100 μM). The 1:0 (*black*) and 1:16 (*red*) are overlaid in the ^{15}N-HSQC spectra. (**B**) ^{15}N-HSQC titration of ^{15}N-Cx45CT with unlabelled CIP75 UBA domain, where the Cx45CT:UBA domain concentration ratios ranged from 1:0 to 1:12.5 and concentration of ^{15}N-Cx45CT remained constant (100 μM). The 1:0 (*black*) and 1:5 (*red*) are overlaid in the ^{15}N-HSQC spectra. (**C**) ^{15}N-HSQC titration of ^{15}N-Cx43CT with unlabelled CIP75 UBA domain, where the Cx43CT:UBA domain concentration ratios ranged from 1:0 to 1:15 and concentration of ^{15}N-Cx45CT remained constant (100 μM). The 1:0 (*black*) and 1:5 (*red*) are overlaid in the ^{15}N-HSQC spectra. Summaries of the residues of (**D**) Cx40CT, (**E**) Cx45CT and (**F**) Cx43CT affected by the CIP75 UBA domain. Residues that completely or mostly disappeared are coloured in green and residues that slightly disappeared or shifted are coloured in yellow. Residues comprising the α-helical areas are underlined with a solid line and residues with a propensity to form an α-helix are underlined with a dashed line.

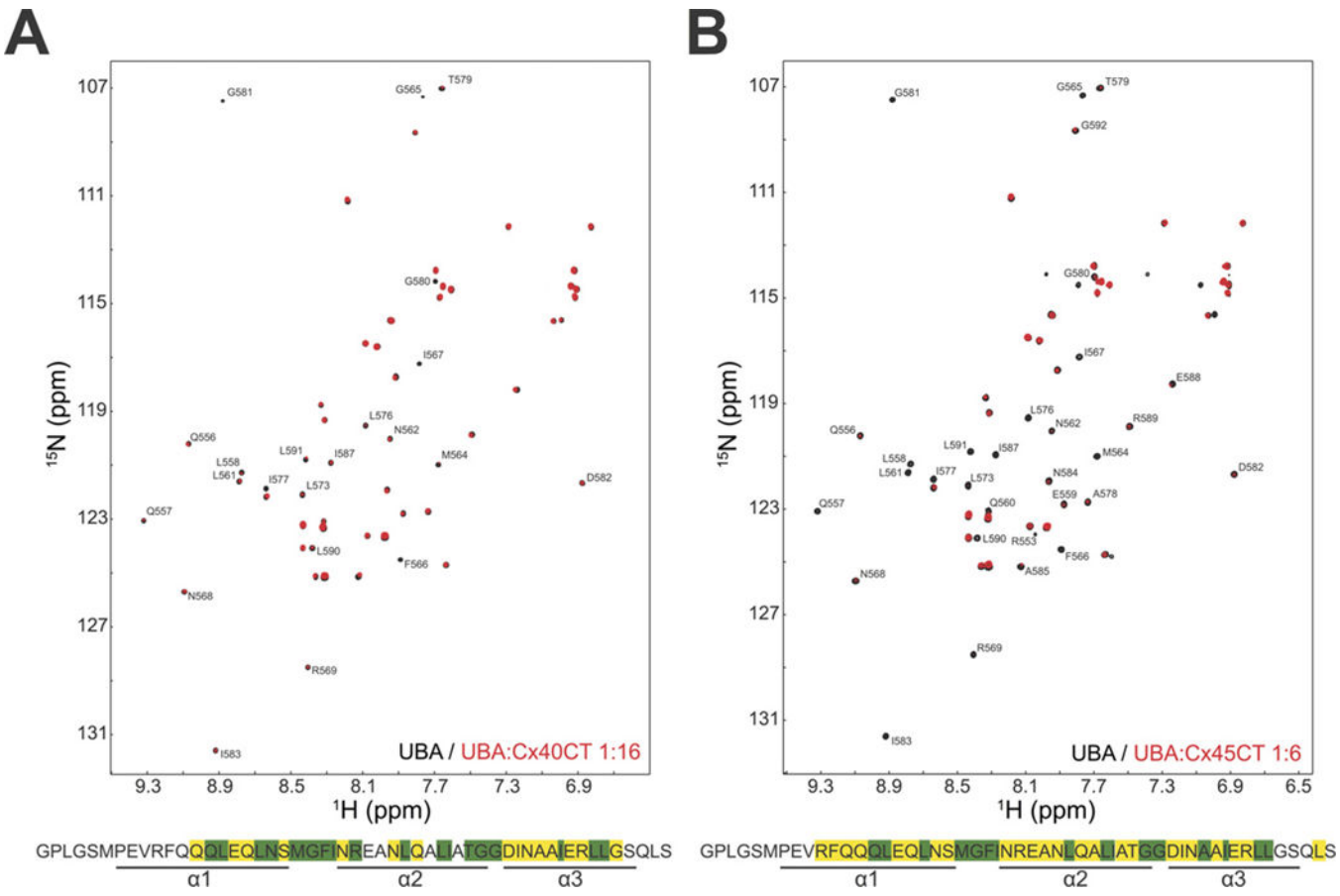

Figure 2. The CIP75 UBA domain directly interacts with Cx40CT and Cx45CT

(**A**) ^{15}N-HSQC titration of ^{15}N-UBA with the unlabelled Cx40CT domain, when the UBA:Cx40CT concentration ratios ranged from 1:0 to 1:16 and the concentration of ^{15}N-UBA remained constant (100 μM). The 1:0 (black) and 1:16 (red) are overlaid in the ^{15}N-HSQC spectra. Titrations of 1:1, 1:2, 1:3, 1:6, 1:8 and 1:12 were also collected (not shown). Lower panel: a summary of all the UBA residues affected by Cx40CT. Residues that completely disappeared are labelled in the ^{15}N-HSQC, all residues that completely or mostly disappeared are coloured in green while residues that slightly disappeared or shifted are coloured in yellow. Residues comprising the three α-helices are underlined. (**B**) ^{15}N-HSQC titration of ^{15}N-UBA with unlabelled Cx45CT domain, which the UBA:Cx45CT concentration ratios ranged from 1:0 to 1:16, and the concentration of ^{15}N-UBA remained constant (100 μM). The 1:0 (black) and 1:6 (red) are overlaid in the ^{15}N-HSQC spectra. Titrations of 1:1, 1:2, 1:3, 1:10, 1:12 and 1:16 were also collected (not shown). Lower panel: a summary of all the UBA residues affected by the presence of Cx45CT, similarly denoted as (**A**), lower panel.

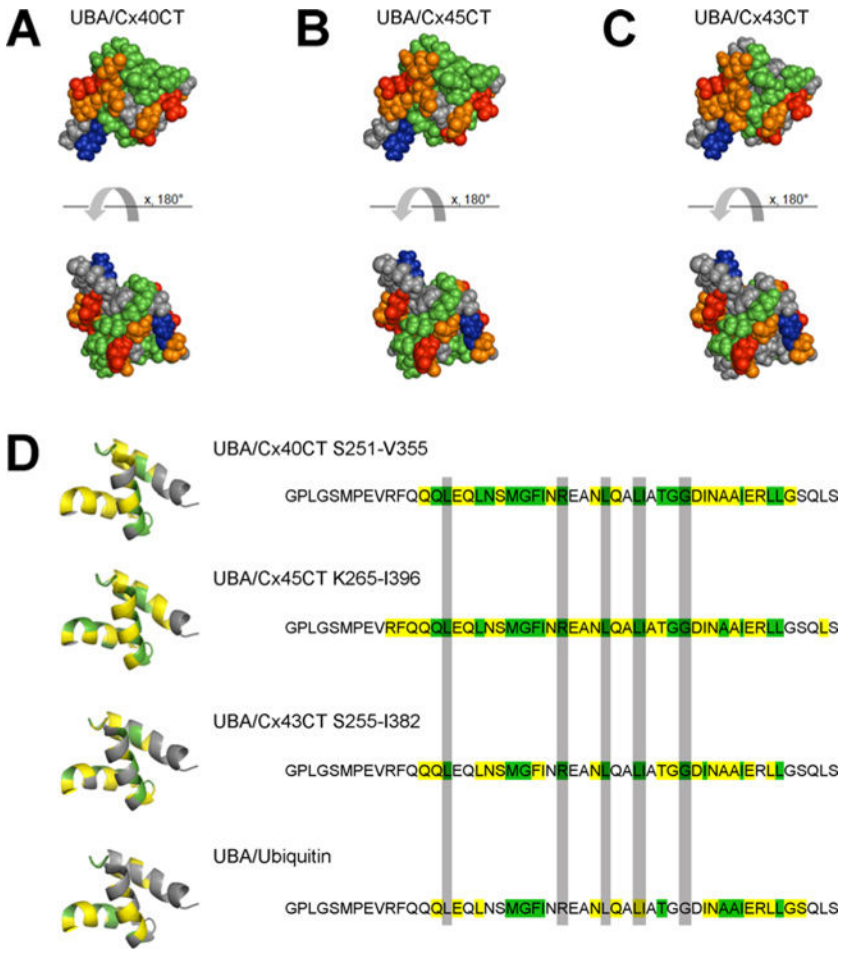

Figure 3. The connexin CT domains, but not ubiquitin, interact with the same region of the CIP75 UBA domain

Hydrophobic surface view of the CIP75 UBA domain (Protein Data Bank code 2KNZ) showing the hydrophobic epitopes 1 and 2. The UBA residues that completely disappeared in the presence of (**A**) Cx40CT, (**B**) Cx45CT or (**C**) Cx43CT are coloured green. Hydrophobic residues (A, G, F, I, L, M, P, V) are coloured grey, negatively charged residues (D, E) in red, positively charged (K, R) in blue, and polar residues (N, Q, S, T, Y, H) in orange. (**D**) For comparison, presented are the ribbon diagram structure and summary of affected residues of CIP75 UBA in the presence of Cx40CT, Cx45CT, Cx43CT or ubiquitin. The UBA/Cx43CT and UBA/ubiquitin interactions were previously published in [26]. Residues that completely disappeared or slightly disappeared/shifted are coloured in green or yellow, respectively. CIP75 UBA domain residues similarly affected by the connexin CT domains, but not ubiquitin, are highlighted in the sequence summary in grey background.

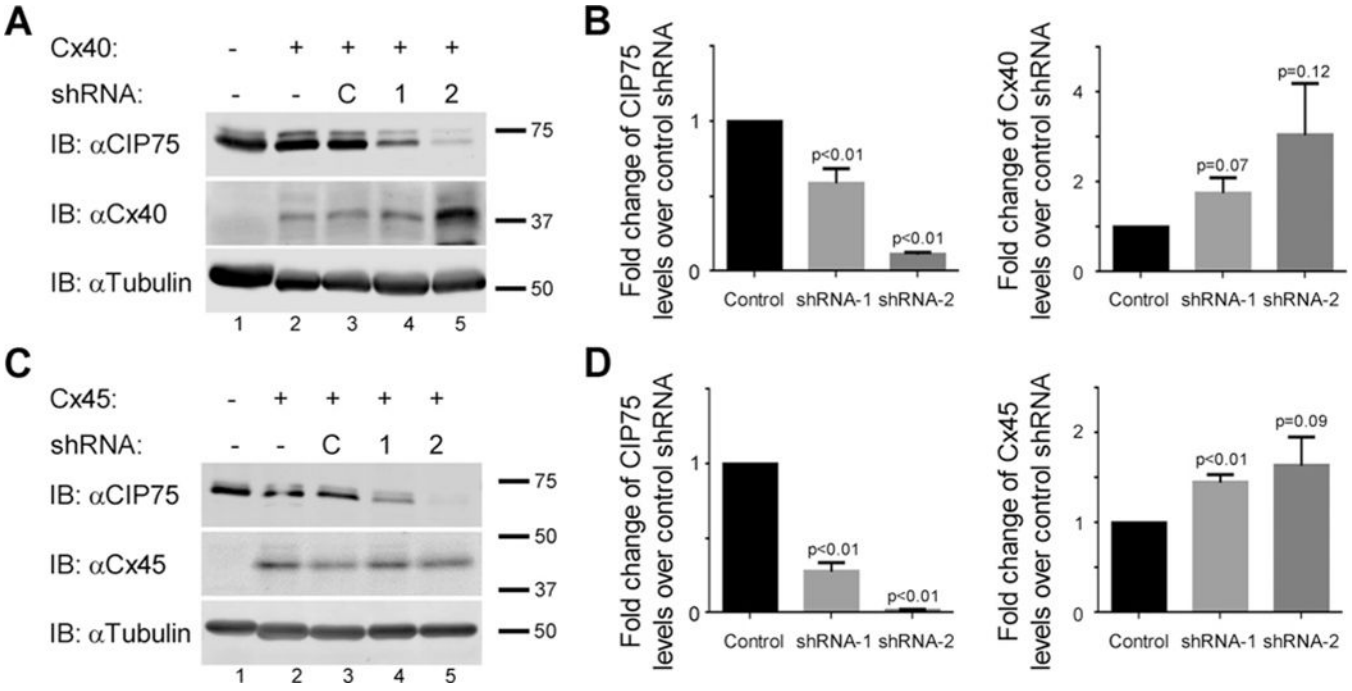

Figure 4. CIP75 regulates Cx40 and Cx45 protein levels

(**A**, **C**) HeLa cells expressing wild-type Cx40 (**A**) or wild-type Cx45 (**C**) were infected with lentivirus containing control ('C') or CIP75 shRNA ('1', '2') expression plasmids. Migration positions of the molecular mass markers (kDa) are indicated at the right of the panels. (**B**, **D**) CIP75 (left panels) and Cx40 (**B**, right panel) or Cx45 (**D**, right panel) levels (normalized to the loading control tubulin) were quantified in control, shRNA-1 and shRNA-2 expressing cells. IB, immunoblot.

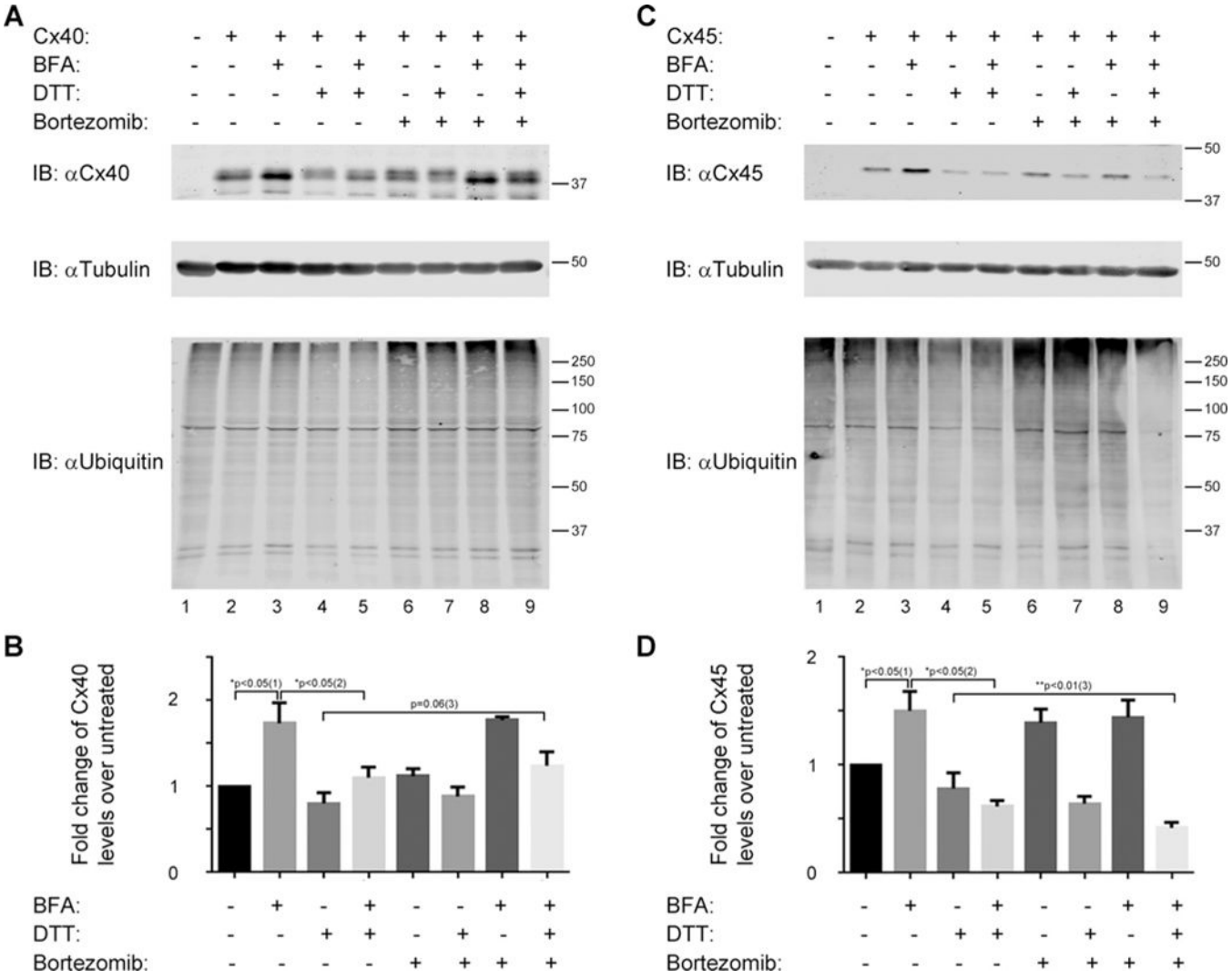

Figure 5. Cx40 and Cx45 are degraded by ERAD

(**A**, **C**) HeLa cells expressing wild-type Cx40 (**A**) or wild-type Cx45 (**C**) were treated with BFA, DTT and bortezomib alone or in combination. Tubulin served as the loading control and ubiquitin confirms a build-up of ubiquitinated proteins as a result of successful proteasomal inhibition. Migration positions of the molecular mass markers (kDa) are indicated at the right of the panels. (**B**, **D**) Cx40 (**B**) or Cx45 (**D**) levels (normalized to tubulin) were quantified in the different treated cells. IP, immunoprecipitation. * and **, statistically significant differences ($P < 0.05$ and $P < 0.01$, respectively) of the change in the amount of total Cx40/Cx45 (1) in BFA-treated cells, (2) in BFA and DTT-treated cells compared with BFA-treated cells, and (3) in BFA, bortezomib and DTT-treated cells compared with DTT-treated cells.

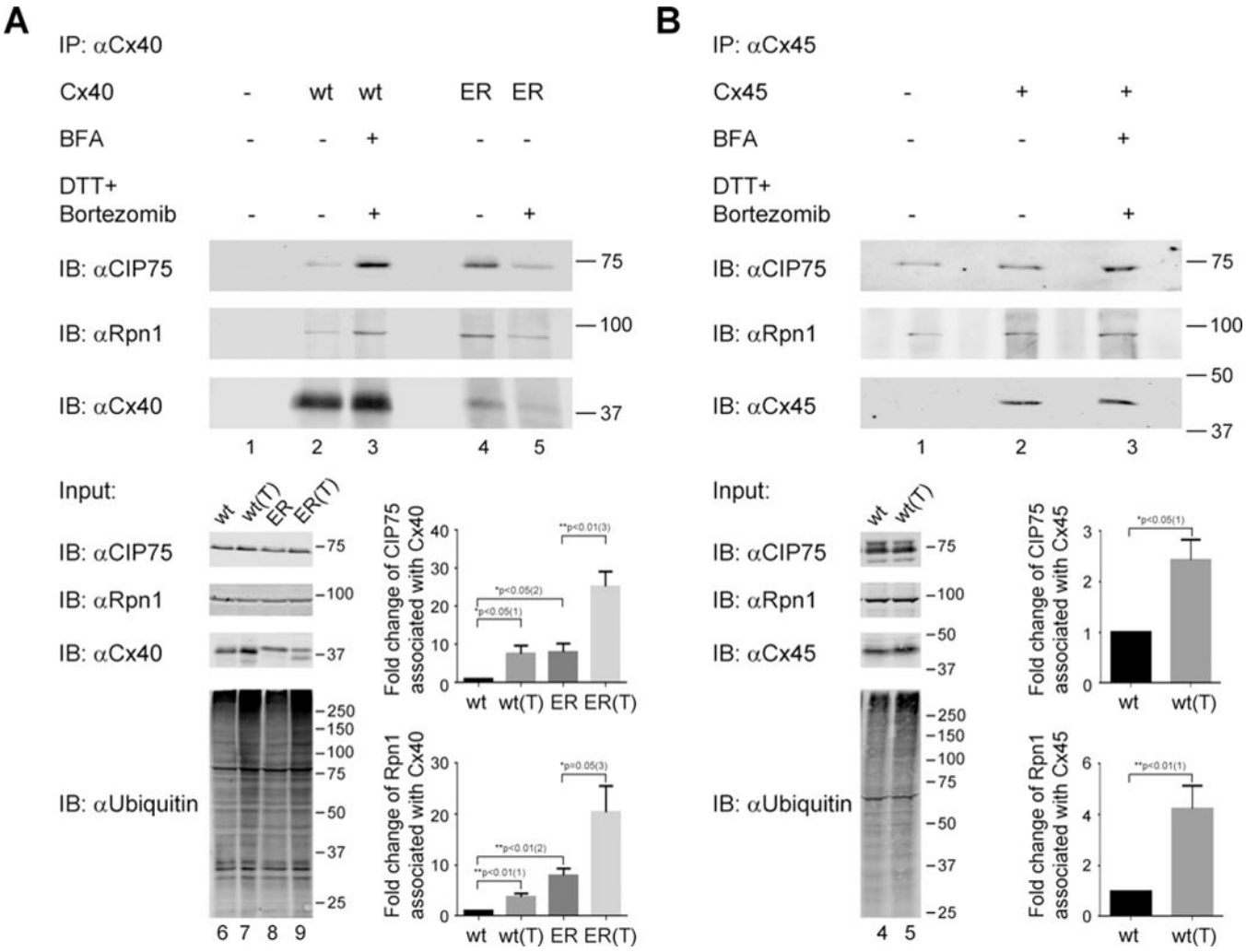

Figure 6. CIP75 and Rpn1 interaction with Cx40 and Cx45 are enhanced under ER-stress conditions

(**A**) Cx40 immunoprecipitation of HeLa-Cx40 (wt) and HeLa-Cx40HKKSL (ER) cells untreated or treated with BFA/bortezomib/DTT (wt) or bortezomib/DTT (ER). (**B**) Cx45 immunoprecipitation of HeLa-Cx45 (wt) cells untreated or treated with BFA/bortezomib/DTT. Input (50 μg) is shown in the bottom left panels (**A** and **B**), where total CIP75 and Rpn1 levels are unchanged by treatment while Cx40, Cx45 and total ubiquitinated proteins have increased levels. Migration positions of the molecular mass markers (kDa) are indicated at the right of the panels. CIP75 and Rpn1 levels found in the co-immunoprecipitation assays relative to immunoprecipitated Cx40 (wt or ER) or Cx45 (wt) were quantified, and represented as the fold change of cells (wt(T), ER, or ER(T)) compared with untreated (wt) cells (bottom right panels for **A** and **B**). Treatment to stimulate ER-stress conditions increases the amount of CIP75 and Rpn1 interacting with ER-localized Cx40 and Cx45. ER-localization alone of Cx40 also increases CIP75 and Rpn1 co-immunoprecipitation compared with wild-type in the untreated cells (wt compared with ER). IP, immunoprecipitation. * and **, statistically significant differences ($P \leq 0.05$ and $P < 0.01$, respectively) of the (1) -fold change in the amount of CIP75 and Rpn1 associated with

wild-type Cx40/Cx45 in BFA, bortezomib and DTT-treated cells compared with the untreated control cells, (2) -fold change in the amount of CIP75 and Rpn1 associated with ER-localized Cx40 compared with wild-type Cx40, and (3) -fold change in the amount of CIP75 and Rpn1 associated with ER-localized Cx40 in bortezomib and DTT-treated cells compared with untreated cells.

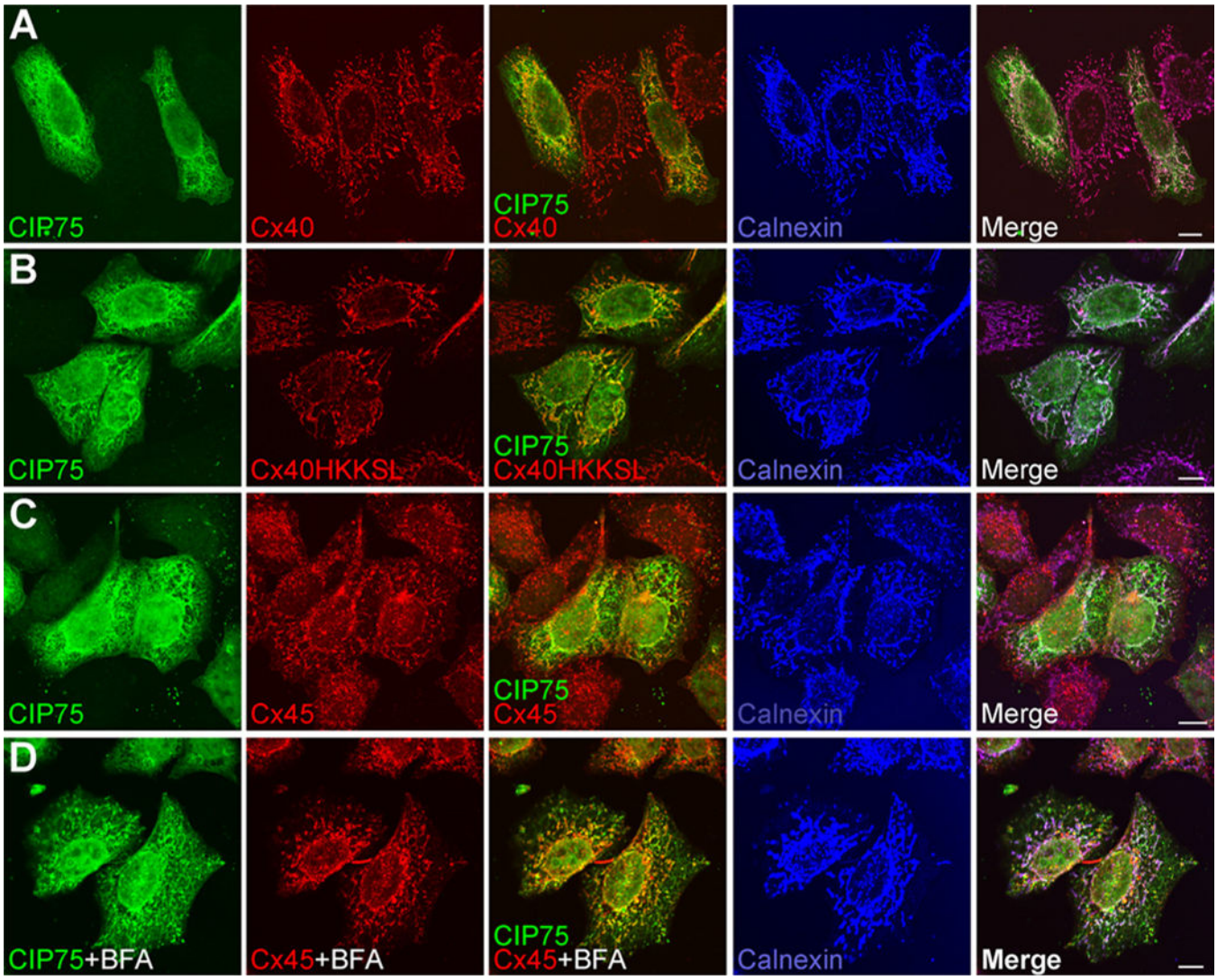

Figure 7. CIP75 co-localizes with Cx40 and Cx45 at the ER

HeLa-Cx40 (**A**), HeLa-Cx40HKKSL (**B**), HeLa-Cx45 (**C** and **D**) cells were transiently transfected with Flag-CIP75. Transfected HeLa-Cx45 cells were also treated with BFA (**D**). The subcellular localization of CIP75 (green) and the connexins (red), with the ER marker calnexin (blue) was visualized by laser scanning confocal microscopy. CIP75 co-localizes with Cx40 and Cx45 (middle panels) at the ER, together with the ER marker calnexin (far right panels). Scale bar: 10 μm.

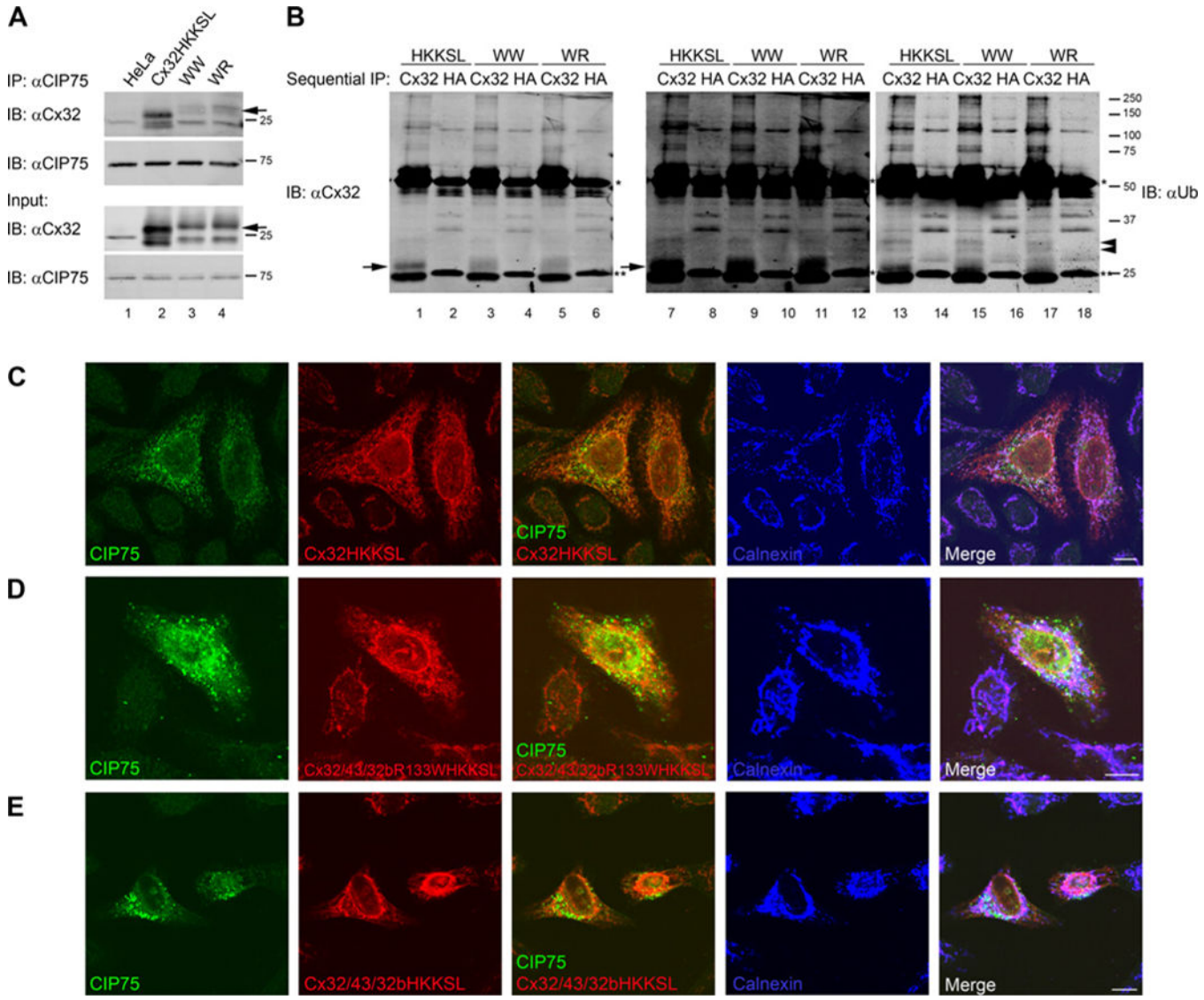

Figure 8. CIP75 interacts with Cx32

(**A**, **B**) HeLa cells were transiently transfected with Cx32HKKSL, Cx32/43/32bR133WHKKSL (WW) or Cx32/43/32bHKKSL (WR). CIP75 immune complexes were initially immunoprecipitated (**A**), followed by a second immunoprecipitation of Cx32 or a non-specific HA IgG control of proteins released from the CIP75 complex (**B**). Sequential immunoprecipitates were blotted for Cx32 (left panel, lanes 1–6 – normal exposure, middle panel, lanes 7–12 – higher exposure) and ubiquitin (right panel, lanes 13–18 – higher exposure). (**A**) Cx32 and the Cx32/43 chimera proteins interact with CIP75 (arrow), (**B**) with slower migrating Cx32 and ubiquitin-positive proteins detected in higher signal blots (middle and right panels, upper 2 arrowheads). * IgG heavy chain and ** light chain. Migration positions of the molecular mass markers in kilodaltons are indicated at the right of the panels. Arrows represent unmodified Cx32-HKKSL or chimeras, arrowheads represent ubiquitinated Cx32-HKKSL or chimeras. (**C**–**E**) HeLa cells were transiently co-transfected with Flag-CIP75 and either Cx32HKKSL,

Cx32/43/32bR133WHKKSL or Cx32/43/32bHKKSL. The subcellular localization of CIP75 (green) and the connexins (red), with the ER marker calnexin (blue) was visualized by laser scanning confocal microscopy. CIP75 co-localizes with Cx32 and the chimeras (middle panels) at the ER, together with the ER marker calnexin (far right panels). Scale bar: 10 μm.

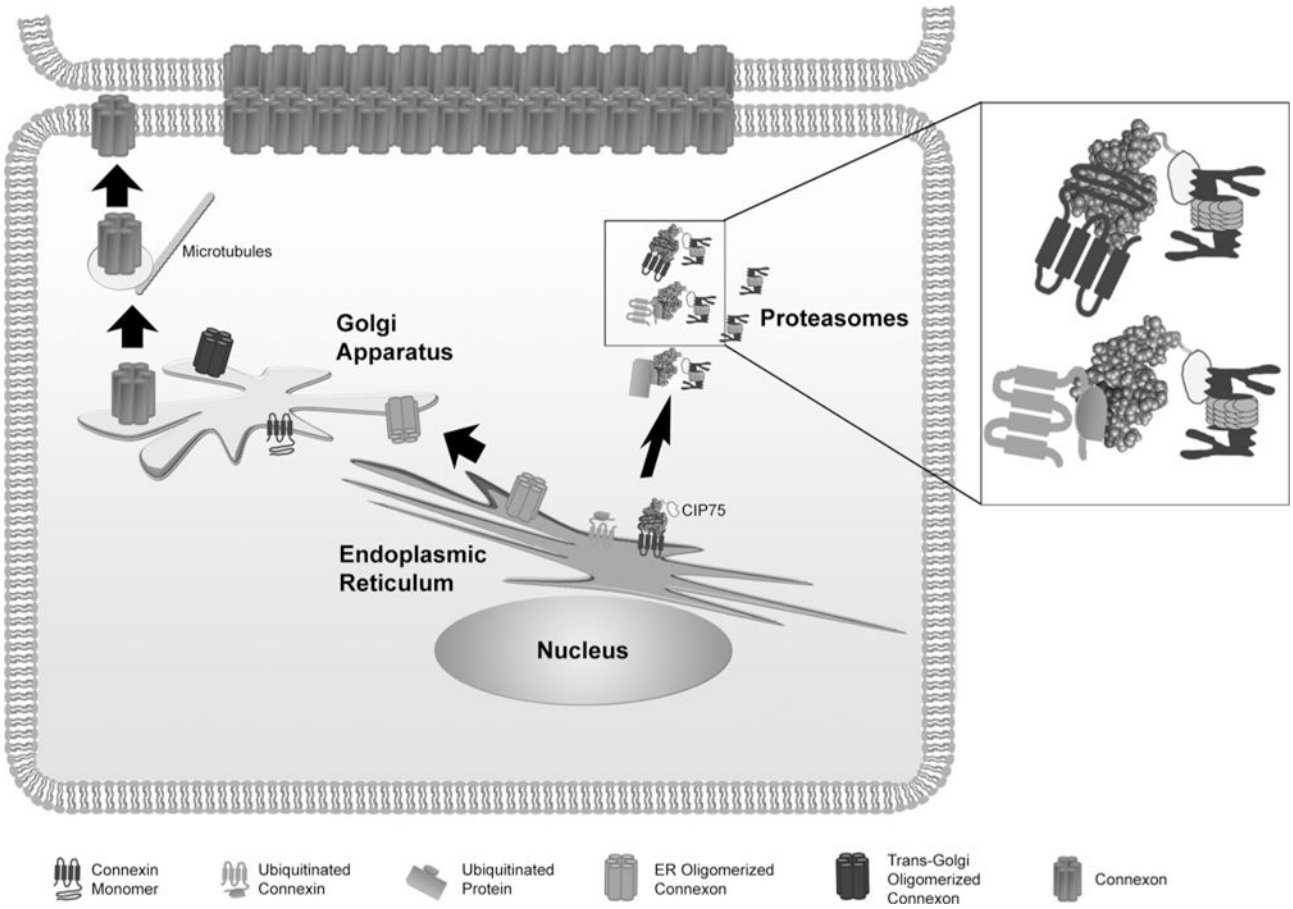

Figure 9. Model for the role of CIP75 in proteasomal degradation via ERAD

CIP75 acts as a shuttle to transport non-ubiquitinated monomeric connexins from the ER membrane to the proteasome for degradation. CIP75 binds to the CT domain of the ER-localized connexin monomer via the UBA domain, aids in translocating the connexin out of the ER membrane into the cytosol and then transports the connexin to the proteasome. There, CIP75 binds to the 19S proteasome cap subunits Rpn1 and Rpn10 via the CIP75 UbL domain, leading to connexin degradation. CIP75 also interacts with ubiquitinated connexins and proteins via the UBA domain, perhaps also facilitating their degradation.